As a result, it is possible to write

$$\frac{\pi^2}{4\sin^2 n'\pi}\int_{-\pi}^{\pi}\sin^2 n'x\,dx=\sum_{n=1}^{\infty}\pi\left|\frac{n}{n^2-n'^2}\right|^2=\pi S'(n') \quad \text{(A8)}$$

and

$$\frac{\pi^2}{4\sin^2 n'\pi}\left(1-\frac{\sin 2n'\pi}{2n'\pi}\right)=S'(n'). \quad \text{(A9)}$$

On inserting expressions for $S'(n')$ and $S'(\frac{1}{2}n')$ from (A9) into Eq. (A5) the desired sum $S(n')$ becomes a complicated trigonometric function of $2n'\pi$, $n'\pi$, and $n'\pi/2$. With the aid of standard trigometric identities, it is possible to reduce this and to show that

$$S(n')=\tfrac{1}{2}\pi^2. \quad \text{(A10)}$$

This particular treatment holds for any nonintegral value of n', where n' may approach an integral value arbitrarily closely.

PHYSICAL REVIEW VOLUME 153, NUMBER 3 15 JANUARY 1967

Electric Field Effects on the Dielectric Constant of Solids*

DAVID E. ASPNES†
Materials Research Laboratory and Department of Electrical Engineering, University of Illinois, Urbana, Illinois

(Received 30 June 1966)

Calculations of the imaginary part of the dielectric constant of an anisotropic solid in the region of a critical point are used to obtain the real part of the dielectric constant through Kramers-Kronig relations. Changes in the real and imaginary parts of the dielectric constant are expressed in closed form for all four types of critical points. Description of these changes can be made with only two functions. The effect of the finite extent of a band is investigated, and it is shown that previous calculations of the change in the imaginary part of the dielectric constant, based on bands of infinite extent, are valid as long as transitions are restricted to regions near the critical point. Closed-form expressions for the Lorentzian broadening of the changes in the dielectric constants are given in terms of Airy functions of complex argument.

I. INTRODUCTION

WITH the evaluation of certain integrals involving Airy functions, it has been possible to obtain the change in the imaginary part of the dielectric constant or optical absorption caused by the application of an arbitrarily oriented electric field near critical points in solids.[1] The same methods can be applied to evaluate the change in the real part of the dielectric constant near critical points, which formerly had been obtained only by numerical integration about the fundamental absorption threshold[2–4] and about the M_1 critical point in the special case of the field parallel to the negative-mass symmetry axis.[2] It is the purpose of this paper to evaluate the dielectric-constant changes caused by an electric field in closed form for an arbitrarily oriented electric field in an anisotropic solid near all four types of critical points, and to investigate the effects of the finite extent of the energy bands on both the real and imaginary parts of the dielectric constant in the presence of an electric field. The weak-field effective-mass approximation will be used throughout.

Rapid changes in the dielectric constant occur at Van Hove singularities in an energy band, where the gradient of the relative energy, $\nabla_{\mathbf{k}}(E_c-E_v)$, vanishes at some value of $\mathbf{k}$.[5,6] Such singularities are of four types, depending on the band curvature or the signs of the reduced masses in the effective-mass approximation. Assuming quadratic energy surfaces, we take the mass of a conduction-band electron along the axes of symmetry as m_{ex}, m_{ey}, and m_{ez}, and the hole masses along the same axes as m_{hx}, m_{hy}, and m_{hz}. Defining the reduced mass m_i for each coordinate $i=x$, y, and z as

$$m_i=\frac{m_{ei}m_{hi}}{m_{ei}+m_{hi}}, \quad (1)$$

the four different critical points may be defined by the reduced-mass signs[6]:

M_0: m_x, m_y, m_z positive (ellipsoid);

M_1: m_x, m_y positive, m_z negative (saddle point);

M_2: m_x, m_y negative, m_z positive (saddle point);

M_3: m_x, m_y, m_z negative (ellipsoid).

For the two saddle-point singularities M_1 and M_2, the mass of odd sign is conventionally taken as m_z.

* This research was supported by the Advanced Research Projects Agency under Contract SD-131, and by the Rome Air Development Command.

† Now at Brown University, Providence, Rhode Island.

[1] D. E. Aspnes, Phys. Rev. **147**, 554 (1966).

[2] B. O. Seraphin and N. Bottka, Phys. Rev. **145**, 628 (1966).

[3] B. O. Seraphin and N. Bottka, Phys. Rev. **139**, A560 (1965).

[4] K. S. Viswanathan and J. Callaway, Phys. Rev. **143**, 564 (1966).

[5] L. Van Hove, Phys. Rev. **89**, 1184 (1953).

[6] D. Brust, Phys. Rev. **134**, A1337 (1964).

II. THE IMAGINARY PART OF THE DIELECTRIC CONSTANT

The imaginary part of the dielectric constant in a weak electric field near any critical point can be written, in an anisotropic solid and with the usual approximation which neglects the Coulomb interaction between the hole and electron, as[1]

$$\epsilon_2(\omega,\mathcal{E})=\frac{4N^6B}{\pi^4\hbar^2\omega^2}(\theta_x\theta_y\theta_z)^{-1/2}\int d\epsilon_x\int d\epsilon_y\int d\epsilon_z$$
$$\times\mathrm{Ai}^2\left(\frac{-\epsilon_x}{\hbar\theta_x}\right)\mathrm{Ai}^2\left(\frac{-\epsilon_y}{\hbar\theta_y}\right)\mathrm{Ai}^2\left(\frac{-\epsilon_z}{\hbar\theta_z}\right)$$
$$\times\delta(E_g-\hbar\omega+\epsilon_x\,\mathrm{sgn}(m_x)+\epsilon_y\,\mathrm{sgn}(m_y)$$
$$+\epsilon_z\,\mathrm{sgn}(m_z)),\quad(2)$$

where, if $\mu_x=|m_x|$, etc., then for each coordinate i

$$\theta_i^3=e^2\mathcal{E}_i^2/2\hbar\mu_i.\quad(3)$$

$\mathcal{E}_i$ is the field component along the ith symmetry axis, N is the normalization constant of the Airy function defined in Eq. (A1) of the Appendix, and

$$B=n\omega R=\frac{2e^2C_0^2}{m^2ch}\left(\frac{8\mu_x\mu_y\mu_z}{\hbar^3}\right)^{1/2}.\quad(4)$$

B is the anisotropic generalization of the constant B used by Seraphin and Bottka[2] for an isotropic solid, R is the anisotropic generalization of the quantity R defined by Tharmalingam,[7] and C_0^2 is the approximately $\mathbf{k}$-independent part of the momentum matrix element[7,8]:

$$|\langle f|\mathbf{P}|i\rangle|^2=C_0^2|\phi(0)|^2\delta_{\mathbf{k}_i\mathbf{k}_f}.\quad(5)$$

The integration variables ϵ_i are the kinetic energies of the electron-hole pair along the symmetry axes in relative coordinates. The type of threshold is determined by the sign dependence of these variables, as determined by the reduced mass, in the arguments of the delta function. Since the delta function is an even function of its argument, it is obvious that the imaginary parts of the dielectric constant for the M_0 and M_3 edges are related by replacing $(E_g-\hbar\omega)$ with $(\hbar\omega-E_g)$ in the result, and the same relation holds between the M_1 and M_2 thresholds. Therefore, only the M_0 and M_1 thresholds will be considered in detail.

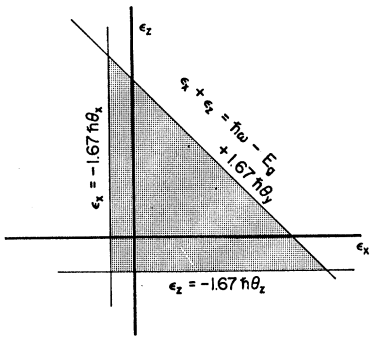

FIG. 1. The closed region of contribution from the integrand of Eq. (2) for the M_0 edge, with $(\hbar\omega-E_g)>0$. The integrand decays exponentially outside this region. The boundaries are taken as those lines where the appropriate limiting Ai^2 factor of the integrand has 0.01 of its value at zero argument.

[7] K. Tharmalingam, Phys. Rev. **130**, 2204 (1963).
[8] R. J. Elliott, Phys. Rev. **108**, 1384 (1957).

The limits on the integrals of Eq. (2) are obtained in the following way. Since the asymptotic limits of the Airy function squared are,[9] for $x\to\infty$,

$$\mathrm{Ai}^2(x)\sim(\pi/4N^2)x^{-1/2}e^{-\frac{4}{3}x^{3/2}},\quad(6a)$$
$$\mathrm{Ai}^2(-x)\sim(\pi/2N^2)x^{-1/2}[1+\sin(\tfrac{4}{3}x^{3/2})],\quad(6b)$$

the lower limits, in which the arguments of the Airy functions become large and positive, can be extended to negative infinity with Eq. (6a) insuring that the Airy functions will cut off the contribution from the integrand for large positive argument. This represents the negative-kinetic-energy region, and picks up the electroabsorption contribution in the nonclassical region of tunnelling. We note from Eqs. (2) and (6) that in the limit of zero field ($\theta_i\to 0$) each Airy function squared reduces to the derivative of the density of states in one dimension: zero below the gap, proportional to $\epsilon_i^{-1/2}$ above.

In principle, the upper limits to the integrals are the maximum kinetic energies of the electron-hole pair, determined by the extent of the relative coordinate electron-hole pair energy band along the particular symmetry axis. This maximum kinetic energy is determined for each coordinate i by

$$E_{i_0}=[(E_c-E_v)_i]_{\max}-E_g,\quad m_i>0\quad(7a)$$
$$=E_g-[(E_c-E_v)_i]_{\min},\quad m_i<0,\quad(7b)$$

where E_g is the energy separation between the valence and conduction bands at the critical point. Because of the delta function of energy and the asymptotic behavior of $\mathrm{Ai}^2(x)$ for positive x, certain cutoff energies may be extended to infinity with negligible error. We consider first the M_0 edge.

Since the delta function requires

$$E_g-\hbar\omega+\epsilon_x+\epsilon_y+\epsilon_z=0\quad(8)$$

for the M_0 edge, the region of contribution of the integrand is bounded because in any direction one of the Airy functions approaches zero as in Eq. (6a). This is illustrated in Fig. 1, where it is assumed that the contributing region is defined as that region where the Airy

[9] H. A. Antosiewicz, in *Handbook of Mathematical Functions*, edited by M. Abramowitz and I. A. Stegun (U. S. Department of Commerce, National Bureau of Standards, Washington, D. C., 1964), Appl. Math. Ser. **55**, p. 448. The Airy functions in the Handbook are normalized to $N=\pi$.

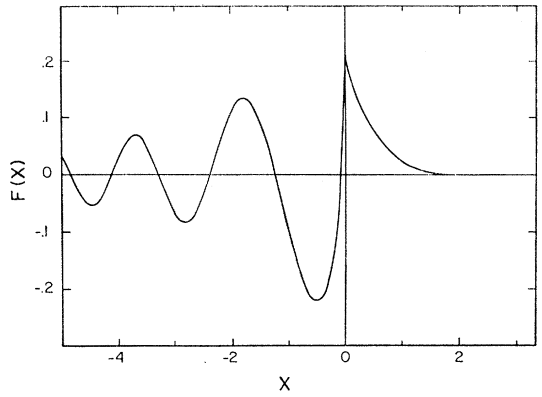

FIG. 2. The electro-optic function $F(x)$.

function arguments are less than $+1.67$, at which point the square of the Airy function has dropped to 0.01 of its value at zero argument. If this region lies within the band, that is, does not extend beyond the upper cutoff energies E_{i_0}, which is true if

$$(\hbar\omega-E_g)<\min(E_{x_0}-1.67(\hbar\theta_y+\hbar\theta_z), E_{y_0}-1.67(\hbar\theta_z+\hbar\theta_x), E_{z_0}-1.67(\hbar\theta_x+\hbar\theta_y)), \quad (9)$$

then all upper limits may be made infinite with negligible error. The integrals can now be evaluated giving[1,7]

$$\epsilon_2(\omega,\mathcal{E})=\frac{B\theta^{1/2}}{\omega^2}\left(\frac{N^2}{\pi}\right)[\mathrm{Ai}'^2(\eta)-\eta\,\mathrm{Ai}^2(\eta)], \quad (10a)$$

$$\eta=(E_g-\hbar\omega)/\hbar\theta, \quad \text{for the } M_0 \text{ edge} \quad (10b)$$

$$=(\hbar\omega-E_g)/\hbar\theta \quad \text{for the } M_3 \text{ edge}. \quad (10c)$$

θ is the generalization of Eq. (3), and is defined in terms of a reduced mass in the direction of the field:

$$\theta^3=e^2\mathcal{E}^2/2\hbar\mu, \quad (11a)$$

where

$$\frac{1}{\mu}=\frac{1}{\mathcal{E}^2}\left[\frac{\mathcal{E}_x^2}{\mu_x}+\frac{\mathcal{E}_y^2}{\mu_y}+\frac{\mathcal{E}_z^2}{\mu_z}\right], \quad (11b)$$

or alternatively,

$$\frac{1}{\mu}=\hbar^{-2}\left|\frac{\partial^2}{\partial k_{\mathrm{rel}\,\parallel}^2}(E_c-E_v)\right|. \quad (11c)$$

The zero-field limit of Eq. (10a) gives the well-known square-root dependence of the density of states

$$\epsilon_2(\omega,0)=(B/\omega^2)\hbar^{-1/2}\times[\pm(\hbar\omega-E_g)]^{1/2}u(\pm(\hbar\omega-E_g)), \quad (12)$$

where $u(x)$ is the unit step function, zero for negative argument and one for positive argument, and where the $+$ sign is taken for M_0 thresholds and the $-$ sign for M_3 edges. The change in the imaginary part of the dielectric constant with applied field is therefore

$$\Delta\epsilon_2(\omega,\mathcal{E})=\epsilon_2(\omega,\mathcal{E})-\epsilon_2(\omega,0) \quad (13a)$$

$$=(B/\omega^2)\theta^{1/2}F(\eta), \quad (13b)$$

where

$$F(\eta)=(N^2/\pi)[\mathrm{Ai}'^2(\eta)-\eta\,\mathrm{Ai}^2(\eta)]-(-\eta)^{1/2}u(-\eta) \quad (14)$$

is the electro-optic function of the first kind, plotted in Fig. 2, and η is given in Eqs. (10b) and (10c) for M_0 and M_3 edges, respectively.

The extension of the upper limits to infinity results in error unless transitions occur only near the critical point, because the bounded region of Fig. 1 may not lie within the band. However, the failure of the assumption of a constant effective mass as transitions occur farther from the critical point will probably define the true region of validity of Eqs. (10). The extension to infinity has also removed the top of the band, so the band appears to extend indefinitely. This causes difficulties in calculating the real part of the dielectric constant with Kramers-Kronig relations. We return to the M_0 and M_3 edges in Sec. III.

The extent in energy of the relative coordinate band plays a much more important part near saddle points, where the sign of one mass is opposite that of the other two. For the M_1 edge, associating the mass of opposite sign with the z-direction, the delta function of Eq. (2) requires

$$E_g-\hbar\omega+\epsilon_x+\epsilon_y-\epsilon_z=0. \quad (15)$$

The major contribution, which comes from the region where no Airy function argument exceeds 1.67, is now obtained from the open region of Fig. 3. Equation (2) is infinite if the region is left open. To close it, we cut off the ϵ_z integral at the maximum kinetic energy allowed in the z direction:

$$E_{z_0}=E_g-(E_c-E_v)_{z_{\min}}>0, \quad \text{for} \quad M_1 \quad (16a)$$

$$=(E_c-E_v)_{z_{\max}}-E_g>0, \quad \text{for} \quad M_2. \quad (16b)$$

As with the M_0 and M_3 edges, we assume that this bounded region lies within the limits in the x and y directions, which occurs if

$$(\hbar\omega-E_g)<\min(E_{x_0}-E_{z_0}-1.67\hbar\theta_y, E_{y_0}-E_{z_0}-1.67\hbar\theta_x). \quad (17)$$

If this is the case the upper limits on the integrals over ϵ_x and ϵ_y can be made infinite with negligible error. Evaluating these integrals gives[1]

$$\epsilon_2(\omega,\mathcal{E})=\frac{BN^3}{\pi^2\hbar\omega^2(\theta_z)^{1/2}}\int_{-\infty}^{E_{z_0}}d\epsilon_z\,\mathrm{Ai}^2\left(\frac{-\epsilon_z}{\hbar\theta_z}\right)\times\mathrm{Ai}_1\left[\kappa\frac{\pm(E_g-\hbar\omega)-\epsilon_z}{\hbar\theta_{xy}}\right], \quad (18a)$$

where

$$\theta_{xy}{}^3=\theta_x{}^3+\theta_y{}^3, \tag{18b}$$

$$\kappa=2^{2/3}, \tag{18c}$$

and

$$\mathrm{Ai}_1(x)=\int_x^\infty dt\,\mathrm{Ai}(t). \tag{18d}$$

The positive sign in Eq. (18a) refers to the M_1 edge, the negative sign to the M_2 threshold. This expression describing the imaginary part of the dielectric constant near a saddle point apparently cannot be evaluated in closed form in general, except in the limit that E_{z_0} becomes infinite, or else that the electric field is parallel to the axis of the mass of opposite sign ($\theta_{xy}=0$). If E_{z_0} becomes infinite, Eq. (18a) also becomes infinite, but the change in ϵ_2 with field can be evaluated and the results of Ref. 1 are obtained. If $\theta_{xy}\to 0$ we make use of the relations describing the asymptotic limits of the integral of the Airy function[10]:

$$\mathrm{Ai}_1(x)\sim\frac{(\pi)^{1/2}}{2N}x^{-3/4}e^{-\frac{2}{3}x^{3/2}}, \tag{19a}$$

$$\mathrm{Ai}_1(-x)\sim\frac{\pi}{N}\left[1-\frac{1}{(\pi)^{1/2}}x^{-3/4}\cos\left(\frac{2}{3}x^{3/2}+\frac{\pi}{4}\right)\right]; \tag{19b}$$

hence, in the limit that $\theta_{xy}\to 0$, the Ai_1 term in Eq. (17) can be treated as either zero or π/N, depending on whether the argument is greater or less than zero. We obtain

$$\epsilon_2(\omega,\mathcal{E}_{11})=\frac{B\theta_z{}^{1/2}}{\omega^2}u\left(\eta+\frac{E_{z_0}}{\hbar\theta_z}\right)\left\{\frac{N^2}{\pi}[\eta\,\mathrm{Ai}^2(\eta)-\mathrm{Ai}'^2(\eta)]\right.$$
$$\left.+\frac{N^2}{\pi}\left[\mathrm{Ai}'^2\left(-\frac{E_{z_0}}{\hbar\theta_z}\right)+\frac{E_{z_0}}{\hbar\theta_z}\mathrm{Ai}^2\left(-\frac{E_{z_0}}{\hbar\theta_z}\right)\right]\right\}, \tag{20a}$$

where

$$\eta=(\hbar\omega-E_g)/\hbar\theta_z, \quad \text{for the } M_1 \text{ edge;} \tag{20b}$$
$$=(E_g-\hbar\omega)/\hbar\theta_z, \quad \text{for the } M_2 \text{ edge.} \tag{20c}$$

The effect of cutting off the hyperbolic band, for the M_1 region as an example, has been to introduce a term of the same form as the leading term, evaluated at the difference between the critical point and minimum separation energies, and also to bring in a unit step function representing the absence of absorption until the minimum separation energy is reached. The zero-field limit can easily be obtained from this through the relations[9]

$$\mathrm{Ai}'^2(x)-x\,\mathrm{Ai}^2(x)\sim 0, \quad \text{if } x>0 \tag{21a}$$
$$\sim(\pi/N^2)(-x)^{1/2}, \quad \text{if } x<0 \tag{21b}$$

or directly from Eq. (18a), and is

$$\epsilon_2(\omega,0)=(B/\omega^2\hbar^{1/2})u(\hbar\theta_z\eta+E_{z_0})$$
$$\times\{(E_{z_0})^{1/2}-(-\hbar\theta_z\eta)^{1/2}u(-\hbar\theta_z\eta)\}, \tag{22}$$

[10] Reference 9, p. 449.

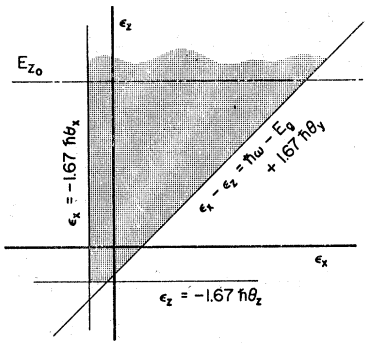

FIG. 3. The open region of contribution from the integrand of Eq. (2) for the M_1 edge, with $(\hbar\omega-E_g)<0$. The integrand decays exponentially outside this region. The boundaries are taken as those lines where the limiting Ai^2 factor of the integrand has 0.01 of its value at zero argument. The cutoff shown for ϵ_z represents the maximum kinetic energy of the electron-hole pair along the negative mass axis.

where η is given in Eqs. (20b) and (20c). Equation (22) is proportional to the density of states for the saddle-point threshold divided by ω^2; the density of states for the M_1 threshold is zero until the minimum energy separation is reached, then rises as a square root and reaches the critical point with infinite slope and becomes constant for higher energies.[6] There is again no top to this band since the extension of the ϵ_x and ϵ_y limits to infinity removed this from the model.

In general, the effect of the ϵ_z kinetic-energy cutoff is to remove the nonphysical infinity in ϵ_2 which arises if this cutoff is not assumed. Correction terms are also obtained which are negligible except when $\hbar\omega$ is within several $\hbar\theta_z$ of $(E_g-E_{z_0})$, so the results obtained for the change in ϵ_2 with no cutoff[1] are generally valid. Equation (18a) can be written as

$$\epsilon_2(\omega,\mathcal{E})=\frac{BN^3}{\pi^2\hbar\omega^2(\theta_z)^{1/2}}$$
$$\times\left\{\int_{-\infty}^{\infty}d\epsilon_z\,\mathrm{Ai}^2\left(\frac{-\epsilon_z}{\hbar\theta_z}\right)\mathrm{Ai}_1\left(\kappa\frac{E_g-\hbar\omega-\epsilon_z}{\hbar\theta_{xy}}\right)\right.$$
$$\left.-\int_{E_{z_0}}^{\infty}d\epsilon_z\,\mathrm{Ai}^2\left(\frac{-\epsilon_z}{\hbar\theta_z}\right)\mathrm{Ai}_1\left(\kappa\frac{E_g-\hbar\omega-\epsilon_z}{\hbar\theta_{xy}}\right)\right\} \tag{23}$$

for the M_1 edge, where the second integral is the correction caused by the finite extent of the band. Both integrals diverge as the square root of the upper limit but these divergences cancel identically. The first integral can be done exactly, and with the first terms of an asymptotic expansion for large E_{z_0} for the second integral, ϵ_2 can be written as

$$\epsilon_2(\omega,\mathcal{E})=\frac{B\theta^{1/2}}{\omega^2}\left\{\frac{N^2}{\pi}[\eta\,\mathrm{Ai}^2(\eta)-\mathrm{Ai}'^2(\eta)]\right.$$
$$\left.+\left(\frac{E_{z_0}}{\hbar\theta}\right)^{1/2}+U\right\}, \quad \text{if } \theta_z>\theta_{xy} \tag{24a}$$

$$\epsilon_2(\omega,\mathfrak{E})=\frac{B\theta^{1/2}}{\omega^2}\left\{\frac{N^2}{\pi}[\eta\,\mathrm{Ai}(-\eta)\,\mathrm{Bi}(-\eta)+\mathrm{Ai}'(-\eta)\,\mathrm{Bi}'(-\eta)]+\left(\frac{E_{z0}}{\hbar\theta}\right)^{1/2}+U\right\},$$

$$\text{if}\quad \theta_{xy}>\theta_z, \tag{24b}$$

where

$$\eta=(\hbar\omega-E_g)/\hbar\theta, \quad \text{for the } M_1 \text{ edge} \tag{25a}$$

$$=(E_g-\hbar\omega)/\hbar\theta, \quad \text{for the } M_2 \text{ edge} \tag{25b}$$

and

$$\theta^3=|\theta_x^3+\theta_y^3-\theta_z^3|. \tag{25c}$$

If $\hbar\omega>E_g-E_{z_0}$ for the M_1 region and $\hbar\omega<E_g+E_{z_0}$ for the M_2 region, the correction term U in Eqs. (24) is

$$U\sim-\frac{1}{4}\left(\frac{\theta_z}{\theta}\right)^{1/2}\left(\frac{\hbar\theta_z}{E_{z_0}}\right)\cos\left[\frac{4}{3}\left(\frac{E_{z_0}}{\hbar\theta_z}\right)^{3/2}\right]-\frac{1}{2\kappa}\left(\frac{\hbar\theta_{xy}^2}{\theta E_{z_0}}\right)^{1/2}\left[\kappa\left(\frac{E_{z_0}}{\hbar\theta_{xy}}-\eta\right)\right]^{-5/4}\times\sin\left[\frac{4}{3}\left(\frac{E_{z_0}}{\hbar\theta_{xy}}-\eta\right)^{3/2}+\frac{\pi}{4}\right], \tag{26}$$

where $\kappa=2^{2/3}$. It is seen that as long as $E_{z_0}\gg\hbar\theta$, the correction term is small with respect to the remaining terms, not only for ϵ_2 but also for the change in ϵ_2 with electric field, defined in Eq. (13a):

$$\Delta\epsilon_2(\omega,\mathfrak{E})=-\frac{B\theta^{1/2}}{\omega^2}F(\eta), \quad \text{if} \quad \theta_z>\theta_{xy} \tag{27a}$$

$$=\frac{B\theta^{1/2}}{\omega^2}G(-\eta), \quad \text{if} \quad \theta_{xy}>\theta_z, \tag{27b}$$

where η and θ are defined in Eqs. (25), $F(\eta)$ is the electro-optic function of the first kind given in Eq. (14), and $G(\eta)$ is the electro-optic function of the second kind, defined as

$$G(\eta)=(N^2/\pi)[\mathrm{Ai}'(\eta)\,\mathrm{Bi}'(\eta)-\eta\,\mathrm{Ai}(\eta)\,\mathrm{Bi}(\eta)]+(\eta)^{1/2}u(\eta); \tag{28}$$

$G(x)$ is plotted in Fig. 4.

It is assumed that the correction term given in Eq. (26) is negligible in regions of interest near the critical point where the effective-mass approximation holds, and that Eqs. (24) with $U=0$, and Eqs. (27) describe both the imaginary part and the change in the imaginary part of the dielectric constant in the presence of an electric field. These expressions will be used to obtain the real part of the dielectric constant through the Kramers-Kronig relations.

Phillips has obtained an expression for the imaginary part of the dielectric constant near an M_1 saddle point

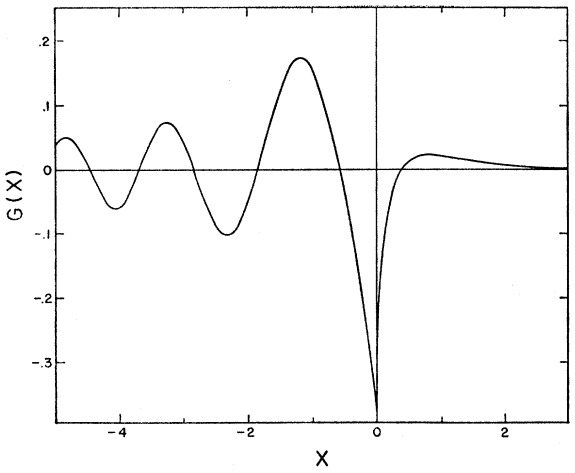

FIG. 4. The electro-optic function $G(x)$.

if the field is parallel to a positive-mass axis[11] which differs from the corresponding result given by Eq. (24b) with $\theta_x=\theta_z=0$. Although Phillips leaves his expression in in the form of an integral, it appears that the oscillatory term will be multiplied by a logarithmic factor which is dependent on the cutoff energy assumed; that is, the magnitude of the oscillations is larger for wider bands. To resolve this discrepancy, we consider Phillips's method of evaluation applied to Eq. (2) for this particular case of $\theta_x=\theta_z=0$. By Eqs. (6), Eq. (2) becomes

$$\epsilon_2(\omega,\mathfrak{E})=\frac{BN^2}{\pi^2\hbar\omega^2\theta_y^{1/2}}\int_0^{E_{x_0}}\frac{d\epsilon_x}{(\epsilon_x)^{1/2}}\int_0^{E_{z_0}}\frac{d\epsilon_z}{(\epsilon_z)^{1/2}}\times\int_{-\infty}^{E_{y_0}}d\epsilon_y\,\mathrm{Ai}^2\left(\frac{-\epsilon_y}{\hbar\theta_y}\right)\delta(E_g-\hbar\omega+\epsilon_x+\epsilon_y-\epsilon_z). \tag{29}$$

Making the usual assumption that $E_{y_0}-E_{z_0}>\hbar\omega-E_g$, so there is no difficulty in carrying out the delta-function integration over ϵ_y, we obtain

$$\epsilon_2(\omega,\mathfrak{E})=\frac{BN^2}{\pi^2\hbar\omega^2\theta_y^{1/2}}\int_0^{E_{x_0}}\frac{d\epsilon_x}{(\epsilon_x)^{1/2}}\times\int_0^{E_{z_0}}\frac{d\epsilon_z}{(\epsilon_z)^{1/2}}\mathrm{Ai}^2\left(\frac{E_g-\hbar\omega+\epsilon_x-\epsilon_z}{\hbar\theta_y}\right). \tag{30}$$

Equation (24b) follows by extending the upper limit of the integral over ϵ_x to infinity, which is permissible if $E_{x_0}-E_{z_0}>\hbar\omega-E_g$, then performing the ϵ_x integration explicitly. To proceed along Phillips's derivation, we define the parabolic coordinates u and v by

$$\hbar u=\epsilon_x-\epsilon_z, \tag{31a}$$

$$\hbar v=2(\epsilon_x\epsilon_z)^{1/2}. \tag{31b}$$

The ϵ_x, ϵ_z plane region of integration, the rectangle

[11] J. C. Phillips, Phys. Rev. **146**, 584 (1966).

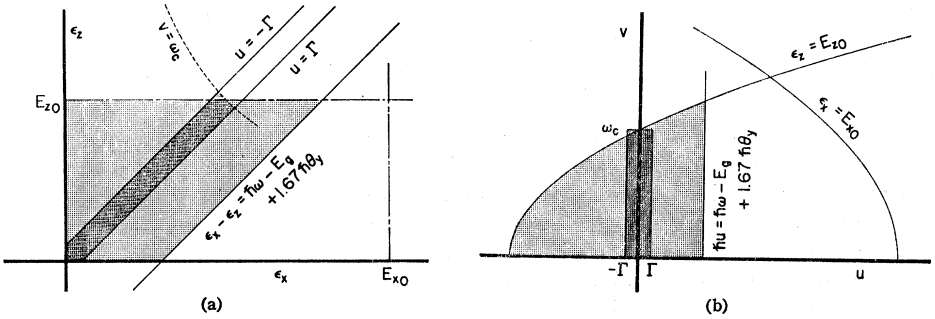

FIG. 5. (a) M_1-edge region of contribution in the ϵ_x, ϵ_z plane. (b) M_1-edge region of contribution in the u, v plane.

$0\leq\epsilon_x\leq E_{x_0}$, $0\leq\epsilon_z\leq E_{z_0}$ shown in Fig. 5(a), becomes the region bounded by the u axis and the two parabolas

$$u=(\hbar/4E_{z_0})v^2-E_{z_0}/\hbar\,, \tag{32a}$$

$$u=-(\hbar/4E_{x_0})v^2+E_{x_0}/\hbar \tag{32b}$$

shown in Fig. 5(b).

The Airy function properties insure essentially no contribution from the region defined by $\hbar u>\hbar\omega-E_g+1.67\hbar\theta_y$; in this case we extend the integral to infinity and Eq. (30) becomes

$$\epsilon_2(\omega,\mathcal{E})=\frac{BN^2}{\pi^2\omega^2\theta_y^{1/2}}\int_{-E_{z_0}/\hbar}^{\infty}du \times\int_0^{[(4E_{z_0}/\hbar)(u+E_{z_0}/\hbar)]^{1/2}}dv\,[u^2+v^2]^{-1/2} \times\mathrm{Ai}^2\left(\frac{E_g-\hbar\omega+\hbar u}{\hbar\theta_y}\right), \tag{33}$$

which is Phillips's Eq. (2.20).

Extending the u limit to infinity eliminates the right-hand parabola bounding the u-v region in Fig. 5(b) and expresses the integral over v in terms of only one boundary. Equation (30) then yields Eq. (24b). Phillips makes a strip approximation by including only the region around $u=0$ defined by $|u|\leq\Gamma$, $0\leq v\leq\omega_c=2E_{z_0}/\hbar$, where Γ is several times the lifetime broadening or the period of the Airy function. This picks up only a part of the contributing region, which becomes the shaded region in the ϵ_x, ϵ_z plane of Fig. 5(a). If $\Gamma\ll\omega_c$, Eq. (33) becomes

$$\epsilon_2=\frac{BN^2}{\pi^2\omega^2\theta_y^{1/2}}\int_{-\Gamma}^{\Gamma}du\,\mathrm{Ai}^2\left(\frac{E_g-\hbar\omega}{\hbar\theta_y}+\frac{u}{\theta_y}\right)\ln\left|\frac{2\omega_c}{u}\right|, \tag{34}$$

which is Phillips' result.

The only real difference between Eqs. (24b) and (34) is the regions of integration that they cover, hence the question of which is the better approximation reduces to that of which area is the better approximation to the electron-hole-pair relative energy band. Since the rectangular area is probably the better approximation, Eq. (24b) should give more accurate results. We consider this in more detail.

The fact that the region of integration for Eq. (34) is smaller shows up in several ways. First, in the zero-field limit, ϵ_2 by Eq. (34) is zero until $\hbar\omega-E_g>-\hbar\Gamma$, in contrast to $\hbar\omega-E_g>-E_{z_0}$ for Eq. (24b). Also in the zero-field limit, if $\hbar\omega-E_g\gg\hbar\Gamma$, Eq. (34) reduces approximately to

$$\epsilon_2=\frac{B}{\pi\omega^2}\left\{\frac{(\hbar)^{1/2}}{(\hbar\omega-E_g)^{1/2}}[\Gamma\ln 2\omega_c-\Gamma\ln\Gamma+\Gamma]\right\}. \tag{35}$$

The bracketed term, which represents the density of states for the saddle-point edge and should be constant in this range of ω,[6] as is the density of states derived from Eq. (24b) in this limit, varies as the inverse square root of $\hbar\omega-E_g$. The smaller region of integration has resulted in an effective loss of $(\hbar\omega-E_g)^{1/2}$ in the density of states. This loss is also apparent if the term $\ln|2\omega_c/u|$ in Eq. (34) is broken up as $[\ln 2\omega_c-\ln|u|]$: The term involving $\ln 2\omega_c$ can be considered an approximation to the term $(E_{z_0}/\hbar\theta_y)^{1/2}$ in Eq. (24b), which arises from the density of states.

The interpretation of the tern $\ln|2\omega_c/u|$ in Eq. (34) as an amplification factor is unrealistic in that the field-dependent oscillations in ϵ_2 arise from two sources, the boundary or cutoff, and the *point* singularity in $|\nabla_{k\,\mathrm{rel}}(E_c-E_v)|^{-1}$. This is true regardless of whether the region in question is elliptical or hyperbolic in nature. The oscillatory term arising from the point singularity should therefore depend solely on band parameters associated with the point singularity itself (E_g, effective masses) and not involve amplification factors dependent on the extent of the band. This is the case for the M_0 and M_3 threshold results given in Eq. (10a), and for the saddle-point results of Eqs. (24). The fact that Γ is small, which is necessary so that the upper limit of the integral over v in Eq. (33) can be replaced by a constant, obscures this in Eq. (34) because of the close proximity of the boundary and the critical point.

III. THE REAL PART OF THE DIELECTRIC CONSTANT

The Kramers-Kronig or dispersion equation[12,13] relates the real and imaginary parts of the dielectric

[12] J. S. Toll, Phys. Rev. **104**, 1760 (1956).
[13] F. Stern, in *Solid State Physics*, edited by F. Seitz and D Turnbull (Academic Press Inc., New York, 1963), Vol. 15, p. 327.

constant:

$$i\pi[\epsilon_1(\omega)-1+i\epsilon_2(\omega)]=\mathcal{P}\int_{-\infty}^{\infty}\frac{\epsilon_1(\omega')-1+i\epsilon_2(\omega')}{\omega'-\omega}d\omega', \quad (36)$$

where $\mathcal{P}$ indicates that the principal part is to be taken. ϵ_2 in Eq. (36) is calculated on the basis of time-dependent perturbation theory which in order to satisfy reality conditions gives two delta functions of energy,[14] $\delta(E_f-E_i-\hbar\omega)$ and $-\delta(E_f-E_i+\hbar\omega)$, only one of which appears in Eq. (2). Since ω ranges over the entire real axis in Eq. (36), it is necessary to include both delta functions which can be done by writing the imaginary part of Eq. (36) as[13]

$$\epsilon_1(\omega,\mathcal{E})=1+\frac{\mathcal{P}}{\pi}\int_{-\infty}^{\infty}\frac{d\omega'}{\omega'-\omega}[\epsilon_2(\omega',\mathcal{E})-\epsilon_2(-\omega',\mathcal{E})], \quad (37)$$

where the functions $\epsilon_2(\omega,\mathcal{E})$ are those derived in the preceding section.

Equation (37) can be converted into the following forms:

$$\epsilon_1(\omega,\mathcal{E})=1+\frac{2}{\pi}\mathcal{P}\int_{-\infty}^{\infty}\frac{\omega'd\omega'\epsilon_2(\omega',\mathcal{E})}{(\omega'+\omega)(\omega'-\omega)} \quad (38a)$$

$$=1+\frac{1}{\omega^2\pi}\mathcal{P}\int_{-\infty}^{\infty}d\omega'\left[\frac{d}{d\omega'}(\omega'^2\epsilon_2(\omega',\mathcal{E}))\right]\times\ln\frac{\omega'^2}{|\omega'+\omega||\omega'-\omega|}. \quad (38b)$$

Equation (38b) can be obtained from Eq. (38a) with an integration by parts and is precisely the weak-field–limit form given by Viswanathan and Callaway[4] as their Eq. (28). We will use Eq. (38a) to calculate $\epsilon_1(\omega,\mathcal{E})$ from the expressions for $\epsilon_2(\omega,\mathcal{E})$ derived in Sec. II, since it is somewhat easier to apply.

As discussed, the models for the imaginary part of the dielectric constant are incorrect in that the bands are open-ended. But since $\epsilon_2(\omega,\mathcal{E})$ decreases asymptotically as $\omega^{3/2}$ for all thresholds on the least convergent side, it should be possible to get reasonable approximations for $\epsilon_1(\omega,\mathcal{E})$ near the critical point; the approximations should be much better for the change in dielectric constant, which drops off as an oscillating function of envelope $\omega^{5/2}$ for all four critical-point regions on their least convergent side.

The calculations are straightforward for the M_0 edge. By Eqs. (10) and (38a)

$$\epsilon_1(\omega,\mathcal{E})=1+B\theta^{1/2}\left(\frac{N^2}{\pi}\right)\times\int_{E_g/\hbar\theta}^{\infty}dt\frac{2}{\pi}\mathcal{P}\int_{-\infty}^{\infty}\frac{d\omega'\,\mathrm{Ai}^2(t-\omega'/\theta)}{\omega'(\omega'+\omega)(\omega'-\omega)}. \quad (39)$$

The principal-part integral can be evaluated by breaking up the denominator using the method of partial fractions together with Eq. (A8b) from the Appendix. We obtain

$$\epsilon_1(\omega,\mathcal{E})=1-\frac{B\theta^{1/2}}{\omega^2}\left\{\frac{N^2}{\pi}[\mathrm{Ai}'(\alpha)\,\mathrm{Bi}'(\alpha)-\alpha\,\mathrm{Ai}(\alpha)\,\mathrm{Bi}(\alpha)]\right.$$
$$-\frac{N^2}{\pi}[\mathrm{Ai}'(\beta)\,\mathrm{Bi}'(\beta)-\beta\,\mathrm{Ai}(\beta)\,\mathrm{Bi}(\beta)]$$
$$\left.-\frac{N^2}{\pi}[\mathrm{Ai}'(\eta)\,\mathrm{Bi}'(\eta)-\eta\,\mathrm{Ai}(\eta)\,\mathrm{Bi}(\eta)]\right\}, \quad (40)$$

where

$$\alpha=\frac{E_g}{\hbar\theta},\quad \beta=\frac{\hbar\omega+E_g}{\hbar\theta},\quad \eta=\frac{E_g-\hbar\omega}{\hbar\theta}. \quad (41)$$

This form, with terms of argument $E_g/\hbar\theta$ and $(E_g+\hbar\omega)/\hbar\theta$, represents the removal of the nonphysical infinity of the double pole in $\epsilon_2(\omega,\mathcal{E})$ at $\omega=0$ which cannot contribute since there are no free carriers in the semiconductor. The more explicit derivation of the Kramers-Kronig relation by Viswanathan and Callaway[4] shows this clearly.

Since $E_g/\hbar\theta$ and $(E_g+\hbar\omega)/\hbar\theta$ are always very large, the terms with these arguments may be replaced with the asymptotic limit of the expression[15]

$$\mathrm{Ai}'(x)\,\mathrm{Bi}'(x)-x\,\mathrm{Ai}(x)\,\mathrm{Bi}(x)\sim-\frac{\pi}{N^2}(x)^{1/2}\left[1-\frac{0.013888\cdots}{(4/9)x^3}\right], \quad (42)$$

with negligible error. For example, with fields around 10^4 V/cm in Ge, $\hbar\theta=0.010$ eV, $E_g=0.80$ eV, so $E_g/\hbar\theta=80$ for the M_0 edge. The second asymptotic term of argument $E_g/\hbar\theta$ therefore contributes about 10^{-7}, compared to the leading terms of argument $(E_g-\hbar\omega)/\hbar\theta$ which are of order 1 for $\hbar\omega\approx E_g$. We therefore replace the terms of argument $E_g/\hbar\theta$ and $(E_g+\hbar\omega)/\hbar\theta$ with their leading asymptotic terms, and ignore further terms in the asymptotic e ansion even when calculating the change with app d field. The result for the M_0 edge is

$$\epsilon_1(\omega,\mathcal{E})=1+\frac{B\theta^{1/2}}{\omega^2}\left\{2\left(\frac{E_g}{\hbar\theta}\right)^{-\left(\frac{E_g+\hbar\omega}{\hbar\theta}\right)^{1/2}}\right.$$
$$\left.+\frac{N^2}{\pi}[\mathrm{Ai}'(\eta)\,\mathrm{Bi}'(\eta)-\eta\,\mathrm{Ai}(\eta)\,\mathrm{Bi}(\eta)]\right\}, \quad (43a)$$

$$\Delta\epsilon_1(\omega,\mathcal{E})=(B\theta^{1/2}/\omega^2)G(\eta), \quad (43b)$$

[14] L. I. Schiff, *Quantum Mechanics* (McGraw-Hill Book Company, Inc., New York, 1955), p. 246.

[15] Reference 9, p. 449. The factor $(-1)^k$ in the summation of the expression for the asymptotic expansion of $\mathrm{Bi}'(z)$ is incorrect and should be deleted [Eq. (10.4.66)].

where

$$\eta=(E_g-\hbar\omega)/\hbar\theta \tag{44}$$

and $G(\eta)$ is given by Eq. (28).

We note that $\Delta\epsilon_1(\omega,\mathcal{E})$ could be obtained by using the approximate dispersion relation on the expression for $\Delta\epsilon_2(\omega,\mathcal{E})$ given by Eq. (13b):

$$\Delta\epsilon_1(\omega,\mathcal{E})\approx\frac{1}{\pi\omega^2}\mathcal{P}\int_{-\infty}^{\infty}\frac{d\omega'}{\omega'-\omega}\omega'^2\Delta\epsilon_2(\omega',\mathcal{E}). \tag{45}$$

This is the dispersion relation used by Seraphin and Bottka in their calculations.[2,3] It is obtained from Eq. (38a) by keeping only the pole $(\omega'-\omega)$ in a partial-fraction expansion. The terms of argument $E_g/\hbar\theta$ and $(E_g+\hbar\omega)/\hbar\theta$ are eliminated with this expression, which means $\Delta\epsilon_1(\omega,\mathcal{E})$ will diverge at $\omega=0$, but near the critical point the approximation is very good. The gap energy E_g now enters only as $(E_g-\hbar\omega)/\hbar\theta$. This explains why Seraphin and Bottka were unable to find any other dependence on E_g in their numerical calculations. Equation (43b) is the closed expression describing the results of their numerical integration.

Equation (38a) can be applied to the M_3 edge and we obtain

$$\begin{aligned}\epsilon_1(\omega,\mathcal{E})=1&\\ +\frac{B\theta^{1/2}}{\omega^2}\Big\{&\frac{2N^2}{\pi}[\mathrm{Ai}'(-\alpha)\,\mathrm{Bi}'(-\alpha)+\alpha\,\mathrm{Ai}(-\alpha)\,\mathrm{Bi}(-\alpha)]\\ &-\frac{N^2}{\pi}[\mathrm{Ai}'(-\beta)\,\mathrm{Bi}'(-\beta)+\beta\,\mathrm{Ai}(-\beta)\,\mathrm{Bi}(-\beta)]\\ &-\frac{N^2}{\pi}[\mathrm{Ai}'(-\eta)\,\mathrm{Bi}'(-\eta)+\eta\,\mathrm{Ai}(-\eta)\,\mathrm{Bi}(-\eta)]\Big\},\end{aligned} \tag{46}$$

where α, β, and η are given in Eq. (41). Terms of argument $E_g/\hbar\theta$ and $(E_g+\hbar\omega)/\hbar\theta$ are now expanded in the large negative-argument asymptotic expansion

$$\mathrm{Ai}'(-x)\,\mathrm{Bi}'(-x)+x\,\mathrm{Ai}(-x)\,\mathrm{Bi}(-x)\sim\frac{\pi}{4N^2x}\sin(\tfrac{4}{3}x^{3/2}). \tag{47}$$

The leading square-root term which appeared for the M_0 edge has vanished; the first asymptotic expansion terms for the M_3 edge are small and can be dropped. Thus, for the M_3 edge, we have

$$\epsilon_1(\omega,\mathcal{E})=1-\frac{B\theta^{1/2}}{\omega^2}\frac{N^2}{\pi}\times[\mathrm{Ai}'(\eta)\,\mathrm{Bi}'(\eta)-\eta\,\mathrm{Ai}(\eta)\,\mathrm{Bi}(\eta)], \tag{48a}$$

$$\Delta\epsilon_1(\omega,\mathcal{E})=-(B\theta^{1/2}/\omega^2)G(\eta), \tag{48b}$$

where η has been redefined to be consistent with Eq. (10c):

$$\eta=(\hbar\omega-E_g)/\hbar\theta. \tag{49}$$

Similar closed-form solutions cannot be obtained for saddle-point thresholds. Application of Eq. (38a) to the expression for the imaginary part of the dielectric constant given by Eq. (18a) yields for the M_1 and M_2 edges, with the help of Eqs. (A8a) and (A13) of the Appendix,

$$\begin{aligned}\epsilon_1(\omega,\mathcal{E})=1\mp&\frac{BN^3}{\pi^2\hbar\omega^2(\theta_z)^{1/2}}\int_{-\infty}^{E_{z_0}}d\epsilon_z\,\mathrm{Ai}^2\Big(\frac{-\epsilon_z}{\hbar\theta_z}\Big)\\ &\times\int_{\mp\kappa(E_g/\hbar\theta_z)}^{\infty}dt\Big\{2\,\mathrm{Gi}\Big(t-\kappa\frac{\epsilon_z}{\hbar\theta_{xy}}\Big)\\ &-\mathrm{Gi}\Big(t+\kappa\frac{-\epsilon_z-\hbar\omega}{\hbar\theta_{xy}}\Big)-\mathrm{Gi}\Big(t+\kappa\frac{-\epsilon_z+\hbar\omega}{\hbar\theta_{xy}}\Big)\Big\}.\end{aligned} \tag{50}$$

The upper signs apply to the M_1 and the lower to the M_2 thresholds, respectively. Equation (50) appears to be integrable in closed form only in the limit that $E_{z_0}\to\infty$, but this leads to a nonphysical negative ϵ_1, depending on the size of B, for the M_2 edge with $\theta_z>\theta_{xy}$. Therefore, it appears that the cutoff E_{z_0} plays an important part in the real part of the dielectric constant near a saddle-point threshold. Since the integral of the Gi function does not have the simple asymptotic forms as the integral of the Ai function, an estimate of the effect of the finite E_{z_0} cannot be obtained. Using the dispersion relation on Eqs. (24) with $U=0$ is equivalent to taking the limit of $E_{z_0}\to\infty$ in Eq. (50); Eqs. (24) with $U=0$ are valid only over the regions $\hbar\omega>E_g-E_{z_0}$ and $\hbar\omega<E_g+E_{z_0}$ for the M_1 and M_2 edges, respectively.

It is expected, however, that the change in the real part of the dielectric constant will be obtained fairly accurately in the region of the critical point by using the approximate dispersion relation given by Eq. (45) on the change in the imaginary part given by Eqs. (27), since $\Delta\epsilon_2(\omega,\mathcal{E})$ drops off rapidly away from the critical point. An alternative derivation is possible by subtracting the zero-field limit of the expression obtained in the evaluation of Eq. (50) in the limit of infinite E_{z_0}. This can be done with relations given in the Appendix. With either method of derivation, the following results are obtained. For the M_1 edge the change in the real part of the dielectric constant takes two forms:

$$\Delta\epsilon_1(\omega,\mathcal{E})=\frac{B\theta^{1/2}}{\omega^2}G\Big(\frac{\hbar\omega-E_g}{\hbar\theta}\Big),\quad\text{if}\quad\theta_z>\theta_{xy} \tag{51a}$$

$$\Delta\epsilon_1(\omega,\mathcal{E})=-\frac{B\theta^{1/2}}{\omega^2}F\Big(\frac{E_g-\hbar\omega}{\hbar\theta}\Big),\quad\text{if}\quad\theta_{xy}>\theta_z. \tag{51b}$$

The M_2 threshold results are

$$\Delta\epsilon_1(\omega,\mathcal{E})=-\frac{B\theta^{1/2}}{\omega^2}G\Big(\frac{E_g-\hbar\omega}{\hbar\theta}\Big),\quad\text{if}\quad\theta_z>\theta_{xy} \tag{52a}$$

$$\Delta\epsilon_1(\omega,\mathcal{E})=\frac{B\theta^{1/2}}{\omega^2}F\Big(\frac{\hbar\omega-E_g}{\hbar\theta}\Big),\quad\text{if}\quad\theta_{xy}>\theta_z. \tag{52b}$$

IV. CONCLUSION

In this paper, the effective-mass weak-field approximation has been used to obtain expressions for the changes of the real and imaginary parts of the dielectric constant near all four types of critical points, in the presence of an electric field oriented in an arbitrary direction in an anisotropic solid. The effects of the finite extent of the bands has been examined, and it has been shown that the previous general treatment,[1] which assumed bands of infinite extent, gives adequate expressions for the changes in the imaginary part of the dielectric constant near the critical points. All changes in the real and imaginary parts of the dielectric constant can be represented either by the electro-optic function of the first kind:

$$F(x)=(N^2/\pi)[\mathrm{Ai}'^2(x)-x\,\mathrm{Ai}^2(x)]-(-x)^{1/2}u(-x) \quad (14)$$

or of the second kind:

$$G(x)=(N^2/\pi)[\mathrm{Ai}'(x)\,\mathrm{Bi}'(x)-x\,\mathrm{Ai}(x)\,\mathrm{Bi}(x)]+(x)^{1/2}u(x), \quad (28)$$

where N is the normalization constant of the Airy function, defined by Eq. (A1) of the Appendix, and $u(x)$ is the unit step function, zero for negative argument and one for positive argument. The electro-optic functions are plotted in Figs. 2 and 4.

The results are summarized in Table I. Quantities used in Table I are listed below for convenience.

$$B=\frac{2e^2C_0^2}{m^2c\hbar}\left(\frac{8\mu_x\mu_y\mu_z}{\hbar^3}\right)^{1/2}, \quad (4)$$

$$\theta_i^3=e^2\mathcal{E}_i^2/2\mu_i\hbar, \quad (3)$$

for each coordinate $i=x$, y, and z.

$$\mu_i=|m_i|=\left|\frac{m_{ei}m_{hi}}{m_{ei}+m_{hi}}\right|, \quad (1)$$

$$\theta_{xy}^3=\theta_x^3+\theta_y^3, \quad (18b)$$

$$\theta^3=e^2\mathcal{E}^2/2\mu\hbar, \quad (11a)$$

where

$$\frac{1}{\mu}=\frac{1}{\mathcal{E}^2}\left[\frac{\mathcal{E}_x^2}{\mu_x}+\frac{\mathcal{E}_y^2}{\mu_y}+\frac{\mathcal{E}_z^2}{\mu_z}\right], \quad (11b)$$

for the M_0 and M_3 thresholds, and

$$\frac{1}{\mu}=\frac{1}{\mathcal{E}^2}\left|\frac{\mathcal{E}_x^2}{\mu_x}+\frac{\mathcal{E}_y^2}{\mu_y}-\frac{\mathcal{E}_z^2}{\mu_z}\right|, \quad (25c)$$

for the M_1 and M_2 regions. The maximum kinetic energy in the direction of the mass of odd sign in the M_1 region is

$$E_{z_0}=E_g-(E_c-E_v)_{\min} \quad (16a)$$

and for the M_2 band:

$$E_{z_0}=(E_c-E_v)_{\max}-E_g. \quad (16b)$$

TABLE I. The dielectric constant $\epsilon(\omega,\mathcal{E})=\epsilon_1(\omega,\mathcal{E})+i\epsilon_2(\omega,\mathcal{E})$ in an electric field, near $M_0(m_x, m_y, m_z>0)$, $M_1(m_x, m_y>0; m_z<0)$, $M_2(m_x, m_y<0; m_z>0)$, and $M_3(m_x, m_y, m_z<0)$ critical points. Constants and functions used in this table are summarized in Sec. IV.

Critical point	η	$\Delta\epsilon_1(\omega,\mathcal{E})$	$\Delta\epsilon_2(\omega,\mathcal{E})$	$\epsilon_2(\omega,\mathcal{E})$	$\epsilon_1(\omega,\mathcal{E})-1$
M_0	$\frac{E_g-\hbar\omega}{\hbar\theta}$	$\frac{B\theta^{1/2}}{\omega^2}G(\eta)$	$\frac{B\theta^{1/2}}{\omega^2}F(\eta)$	$\frac{B\theta^{1/2}N^2}{\omega^2\pi}[\mathrm{Ai}'^2(\eta)-\eta\,\mathrm{Ai}^2(\eta)]$	$\frac{B\theta^{1/2}}{\omega^2}\left\{2\left(\frac{E_g}{\hbar\theta}\right)^{1/2}-\left(\frac{E_g+\hbar\omega}{\hbar\theta}\right)^{1/2}\right\}$ $\frac{N^2}{\pi}+\{-[\mathrm{Ai}'(\eta)\,\mathrm{Bi}'(\eta)-\eta\,\mathrm{Ai}(\eta)\,\mathrm{Bi}(\eta)]\}$
M_1 parallel $\theta_z>\theta_{xy}$	$\frac{\hbar\omega-E_g}{\hbar\theta}$	$\frac{B\theta^{1/2}}{\omega^2}G(\eta)$	$-\frac{B\theta^{1/2}}{\omega^2}F(\eta)$	$\frac{B\theta^{1/2}N^2}{\omega^2\pi}\{-[\eta\,\mathrm{Ai}^2(\eta)-\mathrm{Ai}'^2(\eta)]+\left(\frac{E_z}{\hbar\theta}\right)^{1/2}\}$	$\hbar\omega>E_g-E_{z_0}$ ...
M_1 transverse $\theta_{xy}>\theta_z$	$\frac{E_g-\hbar\omega}{\hbar\theta}$	$\frac{B\theta^{1/2}}{\omega^2}F(\eta)$	$-\frac{B\theta^{1/2}}{\omega^2}G(\eta)$	$\frac{B\theta^{1/2}N^2}{\omega^2\pi}\{-[\mathrm{Ai}'(\eta)\,\mathrm{Bi}'(\eta)-\eta\,\mathrm{Ai}(\eta)\,\mathrm{Bi}(\eta)]+\left(\frac{E_{z_0}}{\hbar\theta}\right)^{1/2}\}$	$\hbar\omega>E_g-E_{z_0}$ ...
M_2 parallel $\theta_z>\theta_{xy}$	$\frac{E_g-\hbar\omega}{\hbar\theta}$	$\frac{B\theta^{1/2}}{\omega^2}G(\eta)$	$-\frac{B\theta^{1/2}}{\omega^2}F(\eta)$	$\frac{B\theta^{1/2}N^2}{\omega^2\pi}\{-[\eta\,\mathrm{Ai}^2(\eta)-\mathrm{Ai}'^2(\eta)]+\left(\frac{E_{z_0}}{\hbar\theta}\right)^{1/2}\}$	$\hbar\omega<E_g+E_z$ ...
M_2 transverse $\theta_{xy}>\theta_z$	$\frac{\hbar\omega-E_g}{\hbar\theta}$	$\frac{B\theta^{1/2}}{\omega^2}F(\eta)$	$\frac{B\theta^{1/2}}{\omega^2}G(\eta)$	$\frac{B\theta^{1/2}N^2}{\omega^2\pi}\{-[\mathrm{Ai}'(\eta)\,\mathrm{Bi}'(\eta)-\eta\,\mathrm{Ai}(\eta)\,\mathrm{Bi}(\eta)]+\left(\frac{E_{z_0}}{\hbar\theta}\right)^{1/2}\}$	$\hbar\omega<E_g+E_{z_0}$ ...
M_3	$\frac{\hbar\omega-E_g}{\hbar\theta}$	$-\frac{B\theta^{1/2}}{\omega^2}G(\eta)$	$\frac{B\theta^{1/2}}{\omega^2}F(\eta)$	$\frac{B\theta^{1/2}N^2}{\omega^2\pi}[\mathrm{Ai}'^2(\eta)-\eta\,\mathrm{Ai}^2(\eta)]$	$\frac{B\theta^{1/2}N^2}{\omega^2\pi}[-\mathrm{Ai}'(\eta)\,\mathrm{Bi}'(\eta)-\eta\,\mathrm{Ai}(\eta)\,\mathrm{Bi}(\eta)]$ ...

These results do not include exciton effects, which are probably important near M_0 critical points at least.[16] The inclusion of exciton effects causes great difficulties and requires numerical evaluation of the equations. This has recently been treated by Duke and Alferieff[16] for M_0 regions of isotropic reduced mass.

When applying the results to a particular material, it is necessary to calculate the electro-optic effect for each pair of valence and conduction bands between which a transition can occur. For instance, in silicon the Λ transition is of the M_1 saddle-point type, with M_1 critical points lying on the (111) axes.[17] Therefore, there are eight such points to sum over, each with the same transition energy. This means that for any electric-field orientation there are, in general, four nonequivalent pairs. Both parallel and transverse type electro-optic effects should occur at the Λ transition, depending on the orientation of the field and the magnitudes of the reduced masses at these critical points.

It will be interesting to determine these reduced masses for the common semiconducting materials so that the theory can be compared with experiment.

ACKNOWLEDGMENT

The author is indebted to Professor Paul Handler for several informative discussions.

APPENDIX

We review some basic relations concerning Airy functions before deriving the equations used in Secs. II and III. The integral representation of the Airy function $\mathrm{Ai}(x)$ is[18]

$$\mathrm{Ai}(x)=\frac{1}{N}\int_0^\infty ds\,\cos(\tfrac{1}{3}s^3+xs) \tag{A1a}$$

$$=\frac{1}{2N}\int_{-\infty}^{\infty} ds e^{i\frac{1}{3}s^3+isx}, \tag{A1b}$$

where the normalization constant N is commonly taken as π or $\sqrt{\pi}$. $\mathrm{Ai}(x)$ is the convergent solution of Airy's equation

$$(d^2/dx^2)\,\mathrm{Ai}(x)=x\,\mathrm{Ai}(x), \tag{A2}$$

which has a linearly independent divergent solution $\mathrm{Bi}(x)$. A closely related function is $\mathrm{Gi}(x)$, defined by[18]

$$\mathrm{Gi}(x)=\frac{1}{N}\int_0^\infty ds\,\sin(\tfrac{1}{3}s^3+xs), \tag{A3}$$

and we note that Eqs. (A1a) and (A3) can be combined in the single representation

$$\mathrm{Ai}(x)+i\,\mathrm{Gi}(x)=\frac{1}{N}\int_0^\infty ds e^{i\frac{1}{3}s^3+isx}. \tag{A4}$$

As shown in Ref. 1, the integral representation of the square of the Airy function is

$$\mathrm{Ai}^2(x)=\frac{\sqrt{\pi}}{2N^2}\int_0^\infty \frac{ds}{\sqrt{s}}\cos\left(\frac{1}{12}s^3+xs+\frac{\pi}{4}\right), \tag{A5}$$

and a second closely related integral was shown to represent the function

$$\mathrm{Ai}(x)\,\mathrm{Bi}(x)=\frac{\sqrt{\pi}}{2N^2}\int_0^\infty \frac{ds}{\sqrt{s}}\sin\left(\frac{1}{12}s^3+xs+\frac{\pi}{4}\right). \tag{A6}$$

As with $\mathrm{Ai}(x)$ and $\mathrm{Gi}(x)$, we can combine $\mathrm{Ai}^2(x)$ and $\mathrm{Ai}(x)\,\mathrm{Bi}(x)$ in a single integral representation

$$\mathrm{Ai}^2(x)+i\,\mathrm{Ai}(x)\,\mathrm{Bi}(x)=\frac{\sqrt{\pi}}{2N^2}\int_0^\infty \frac{ds}{\sqrt{s}}e^{i(1/12)s^3+ixs+i(\pi/4)}. \tag{A7}$$

Both representations of Eqs. (A4) and (A7) can be analytically continued into the upper half of the complex plane. Moreover, the functions $f_1(z)=\mathrm{Ai}(z)+i\,\mathrm{Gi}(z)$ and $f_2(z)=\mathrm{Ai}^2(z)+i\,\mathrm{Ai}(z)\,\mathrm{Bi}(z)$ are analytic throughout this region, which includes the real axis, and by their integral representations they approach zero exponentially as the magnitude of z goes to infinity in the upper half-plane. An integral over the upper half-plane infinite arc therefore vanishes. Since the functions are analytic in this region, their real and imaginary parts are related by the Kramers-Kronig integral[12]:

$$i\pi[\mathrm{Ai}(x)+i\,\mathrm{Gi}(x)]=\mathcal{P}\int_{-\infty}^{\infty} dx'\frac{\mathrm{Ai}(x')+i\,\mathrm{Gi}(x')}{x'-x}, \tag{A8a}$$

$$i\pi[\mathrm{Ai}^2(x)+i\,\mathrm{Ai}(x)\,\mathrm{Bi}(x)]=\mathcal{P}\int_{-\infty}^{\infty} dx'\frac{\mathrm{Ai}^2(x')+i\,\mathrm{Ai}(x')\,\mathrm{Bi}(x')}{x'-x}. \tag{A8b}$$

These equations can be used to obtain the real part of the dielectric constant from the imaginary part as indicated in Sec. III.

We note an immediate consequence of the vanishing of the integral of $\mathrm{Ai}^2(z)+i\,\mathrm{Ai}(z)\,\mathrm{Bi}(z)$ on the infinite arc of the upper half-plane. Since the electro-optic functions given in Eqs. (14) and (28) can be written

$$H(x)=F(x)+iG(x)=-\frac{N^2}{\pi}\int^x dt[\mathrm{Ai}^2(t)+i\,\mathrm{Ai}(t)\,\mathrm{Bi}(t)]-(-x)^{1/2}u(-x)+i(x)^{1/2}u(x), \tag{A9}$$

[16] C. B. Duke and M. E. Alferieff, Phys. Rev. 145, 583 (1966).
[17] J. C. Phillips, in *Solid State Physics*, edited by F. Seitz and D. Turnbull (Academic Press Inc., New York, 1966), Vol. 18, p. 55.
[18] Reference 9, p. 447.

where $u(x)$ is the unit step function, the Lorentzian broadening of the two kinds of electro-optic functions can be given as the real and imaginary parts of

$$H(x_0,\Gamma)=\frac{\Gamma}{\pi}\int_{-\infty}^{\infty}\frac{H(x)dx}{(x-x_0)^2+\Gamma^2}. \tag{A10}$$

The vanishing of the infinite arc integral enables the integral part of Eq. (A9) to be evaluated as $2\pi i$ times the residue at the upper half-plane pole of Eq. (A10), $z=x_0+i\Gamma$. Since the Lorentzian broadening of $(x)^{1/2}u(x)$ is

$$\frac{\Gamma}{\pi}\int_{-\infty}^{\infty}\frac{(x)^{1/2}u(x)dx}{(x-x_0)^2+\Gamma^2}=\left\{\frac{x_0+(x_0^2+\Gamma^2)^{1/2}}{2}\right\}^{1/2}, \tag{A11}$$

the analytic expressions for the Lorentzian broadening of the electro-optic functions $F(x)$ and $G(x)$ are

$$\begin{aligned}&F(x_0,\Gamma)+iG(x_0,\Gamma)\\&=2(N^2/\pi)[e^{-i(\pi/3)}\,\mathrm{Ai}'(z)\,\mathrm{Ai}'(w)+w\,\mathrm{Ai}(z)\,\mathrm{Ai}(w)]\\&\quad-\left\{\frac{-x_0+(x_0^2+\Gamma^2)^{1/2}}{2}\right\}^{1/2}\\&\qquad+i\left\{\frac{x_0+(x_0^2+\Gamma^2)^{1/2}}{2}\right\}^{1/2},\end{aligned} \tag{A12a}$$

where

$$z=x_0+i\Gamma \tag{A12b}$$

$$=\pm\frac{E_g-\hbar\omega}{\hbar\theta}+i\frac{\Gamma(\text{energy units})}{\hbar\theta}, \tag{A12c}$$

and

$$w=ze^{-(2\pi/3)i}. \tag{A12d}$$

To simplify the result, we have used[19]

$$\mathrm{Ai}(z)+i\,\mathrm{Bi}(z)=2e^{i\pi/3}\,\mathrm{Ai}(w). \tag{A12e}$$

Equation (A12a) is a closed analytic expression for the curves obtained numerically by Seraphin and Bottka,[2] though at the expense of using complex arguments in the Airy functions.

A discussion of the effects of broadening is given in Ref. 2, but it should be mentioned that these curves are slightly in error in that they do not approach zero as $(\hbar\omega-E_g)$ becomes large on the oscillatory side. (All curves except the 15 kV/cm curve in Fig. 7 of Ref. 2 are examples of this.) Application to electroabsorption is given by Hamakawa, Germano, and Handler.[20]

To reduce Eq. (50) in the limit of infinite E_{z_0}, integral relations involving the Gi function are needed. Since these may easily be obtained by the methods of Ref. 1 which were applied to the closely related Ai function, only the results of such derivations are presented. Equations necessary to evaluate Eq. (50) are

$$\int_{-\infty}^{\infty}du\,\mathrm{Gi}(u)\,\mathrm{Ai}(\alpha u+\beta)$$

$$=\frac{\pi}{N(\alpha^3-1)^{1/3}}\mathrm{Gi}\left[\frac{\beta}{(1-\alpha^3)^{1/3}}\right],\quad\text{if}\quad\alpha\neq1 \tag{A13a}$$

$$=-\frac{\pi}{\beta N^2},\quad\text{if}\quad\alpha=1 \tag{A13b}$$

$$\int_0^{\infty}\frac{dr}{\sqrt{r}}\,\mathrm{Gi}(r+\alpha)=\kappa N\,\mathrm{Ai}\left(\frac{\alpha}{-\kappa}\right)\mathrm{Bi}\left(\frac{\alpha}{-\kappa}\right) \tag{A14a}$$

$$\int_0^{\infty}\frac{dr}{\sqrt{r}}\,\mathrm{Gi}(\alpha-r)=-\kappa N\,\mathrm{Ai}^2\left(\frac{\alpha}{-\kappa}\right), \tag{A14b}$$

where $\kappa=2^{2/3}$, and N is the normalization constant of Eq. (A1).

In order to numerically evaluate the derived expressions, the author has generated 9-significant-figure FORTRAN subroutines for $\mathrm{Ai}(x)$, $\mathrm{Ai}'(x)$, $\mathrm{Bi}(x)$, $\mathrm{Bi}'(x)$, $\mathrm{Ai}(x)\,\mathrm{Bi}(x)$, and $\mathrm{Ai}'(x)\,\mathrm{Bi}'(x)$; FORTRAN subroutines for $\mathrm{Ai}(z)$ and $\mathrm{Ai}'(z)$ where z is complex have been developed by D. Blossey of this research laboratory (unpublished).

[19] Reference 9, p. 446.

[20] Y. Hamakawa, F. A. Germano, and P. Handler, in Proceedings of the International Conference on the Physics of Semiconductors, Kyoto, Japan, 1966 (unpublished).